13th World Conference on Earthquake Engineering
Vancouver, B.C., Canada
August 1-6, 2004
Paper No. 2178

PSEUDO-DYNAMIC TESTING OF A FULL-SCALE RCS FRAME: PART 1 – DESIGN, CONSTRUCTION AND TESTING

Chui-Hsin CHEN[1], Wen-Chi LAI[1], Paul CORDOVA[2], Greg DEIERLEIN[3], Keh-Chyuan TSAI[4]

SUMMARY

With the aim to validate the seismic performance of composite moment frame systems, a full-scale three-story composite moment frame was pseudo-dynamically tested under four imposed earthquake inputs of varying hazard levels. Following pseudo-dynamic testing, the frame was subjected to a static push with imposed story drift ratios up to 10%. Overall, the composite test frame exhibited robust seismic behavior and performed to the levels implied by building provisions. This paper reviews the planning, design, construction, and execution of the test including a brief summary of results. Comparisons with analytical simulations and design implications are discussed in a companion paper.

INTRODUCTION

This is the first of a two-part paper describing a pseudo-dynamic test of a full-scale three-story three-bay composite steel concrete frame. Conducted through a collaborative study between researchers in Taiwan and the United States, the test is considered a sequel to the US-Japan program on Composite and Hybrid Structures [1], where the impetus for large-scale testing to validate these systems was first introduced. The test specimen is an RCS moment frame consisting of reinforced concrete (RC) columns with composite steel (S) beams. The frame measures 12 meters tall and 21 meters long, making it among the largest frame tests of its type ever conducted. The three-story prototype building is designed for a highly seismic location representative of conditions in California or Taiwan, following provisions for composite structures in the International Building Code [2] and supporting standards. The frame is loaded pseudo-dynamically using input ground motions from the 1999 Chi-Chi and 1989 Loma Prieta earthquakes, scaled to represent seismic hazards with 50%, 10%, and 2% chance of exceedence in 50 years. Following the pseudo-dynamic tests, the frame was quasi-statically pushed to a maximum interstory story drift ratio of 10 percent, which provides valuable data to validate models to simulate near collapse conditions. This paper reviews the design, construction, and testing of the composite RCS frame. Reported test results include overall and component load-deformation response and observed damage patterns. A second

[1] Research Assistant, National Center for Research in Earthquake Engineering (NCREE), Taiwan; email: chchen@ncree.gov.tw, r90521215@ms90.ntu.edu.tw
[2] Research Assistant, J.A. Blume Earthquake Eng. Center, Stanford Univ., Stanford, CA, USA; e-mail: cordova@stanford.edu
[3] Professor & Director, J.A. Blume Earthquake Eng. Center., Stanford Univ., e-mail: ggd@stanford.edu
[4] Professor, NCREE, Taiwan, e-mail: kctsai@ce.ntu.edu.tw

companion paper (Cordova et al. [3]) focuses on the validation of the analytical simulation models and the resulting design implications from the test.

Advantages of the RCS System

RCS systems were developed about twenty-five years ago as an alternative to conventional all-steel and all-concrete moment frames. The primary motivation behind their development is that the system optimizes the usage of the steel and concrete materials. Reinforced concrete columns offer a significant cost-advantage over structural steel for resisting compressive column loads (Griffis [4]), while composite steel beams and composite slab-deck provides an efficient floor framing system for long spans desired in commercial buildings. Innovative construction (pre-cast or cast-in-place) and staging operations also add to the attractiveness of RCS construction by reducing the cost and construction time.

Perhaps the most significant advantage of this system is the design and performance of the beam-column connection. Shown in Fig. 1 is a typical connection where the steel beam passes continuous through the joint, thereby avoiding interruption of the beam at the column face and eliminating the need for welding or bolting the beam at the point of maximum moment. This type of connection detail avoids the fracture problems of conventional steel moment frames that were encountered during the 1994 Northridge and 1995 Hanshin earthquakes. It also reduces the anchorage and congestion problems often found in reinforced concrete structures. Extensive testing over the last fifteen years has demonstrated that composite connections, when properly detailed, can provide reliable hysteretic behavior and sufficient strength to develop the beam plastic moment. Based on tests conducted by Sheikh [5], Deierlein [6] proposed design equations to quantify the strength and stiffness of composite connections, which were subsequently incorporated a set of ASCE guidelines for design of joints between RC columns and steel beams [7]. Researchers have continued to study these connections and are improving the accuracy and robustness of the ASCE joint model, as is reflected by more recent studies by Kanno and Deierlein [8] and Parra-Montesinos [9].

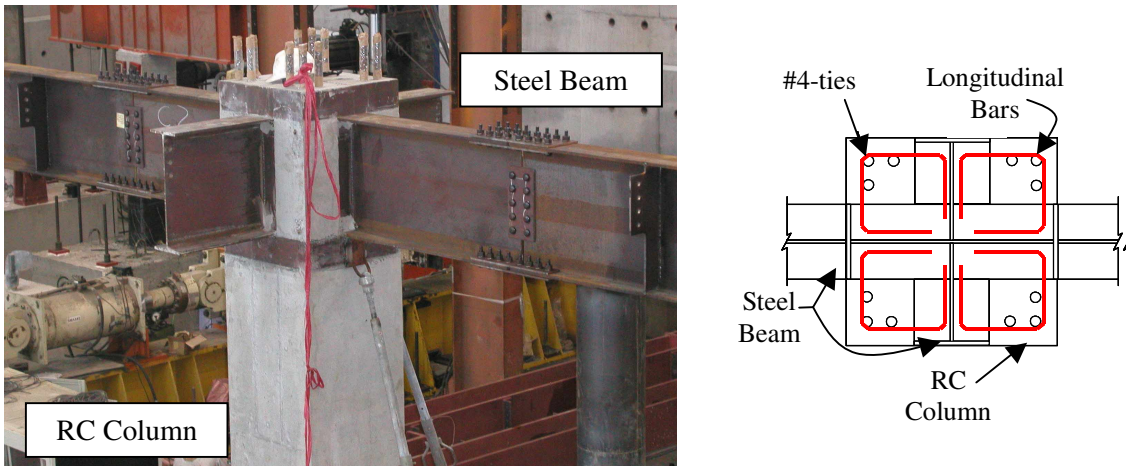

(a) (b)

Figure 1 – (a) Typical RCS composite joint with (b) a transverse beam and square tie details.

System Design Guidelines

Aside from the unique detailing requirements for composite beam-column joints, design provisions for composite frames follow directly from those of conventional reinforced concrete and structural steel construction. The RC columns are designed per ACI-318 [10] and the steel (or composite) beams are

designed by the AISC-LRFD Specification [11]. General seismic loading and design requirements are included in the International Building Code [2] or more recently the SEI/ASCE 7-02 Minimum Design Loads for Buildings and Other Structures [12]. These documents then adopt Part II of the AISC Seismic Design Provisions [13], which outlines specific detailing requirements for RCS frames (composite special moment frames). Further details on the development of these seismic provisions are summarized by Deierlein [14].

Rationale behind Full-Scale Test

While RCS moment frame systems have been used for nearly twenty-five years, most applications in the U.S. have been high-rise buildings in low seismic regions with few inroads to high seismic regions in the western U.S. This is in spite of research (e.g., see [15] and [16]), which has shown the seismic performance of these systems to be at least equivalent to all-steel moment frames; and, it is in contrast to use of RCS systems in high-seismic regions of Japan. The full-scale RCS frame test reported herein is intended as a "proof of concept" to help demonstrate the efficacy of innovative composite moment frames as alternatives to conventional steel and concrete systems in high-seismic regions. In addition, the test will provide important data to evaluate and validate current design provisions and performance-based simulation and assessment technologies for composite moment frames. Design provisions and topics of interest include strong-column weak-beam criterion, composite action of concrete slab and steel beams, integrity of the precast column and composite beam-column connections, and overall frame response. Apart from these direct benefits, the large test provides an impetus to explore international collaboration and data archiving envisioned for the Networked Earthquake Engineering Simulation (NEES) initiative and the Internet-based Simulations for Earthquake Engineering (ISEE) (see [17] and [18]) launched recently in the U.S. and Taiwan, respectively.

PLANNING AND DESIGN OF TEST FRAME

The design, construction, and loading of this test frame are as realistic as possible, subject to practical constraints of the laboratory at the National Center for Research in Earthquake Engineering (NCREE) in Taiwan. The 15-meter tall strong wall and space limitations due to other experiments dictated the maximum size and profile of the test frame. The three-story three-bay RCS test frame, shown in Fig. 2, is based on a rectangular three-story office building with seven-meter bays four-meter story heights. The frame is conceived of in a framing arrangement where the moment resisting frame tested in the lab is assumed to provide lateral support to three tributary bays of framing (equivalent to a tributary area of 588

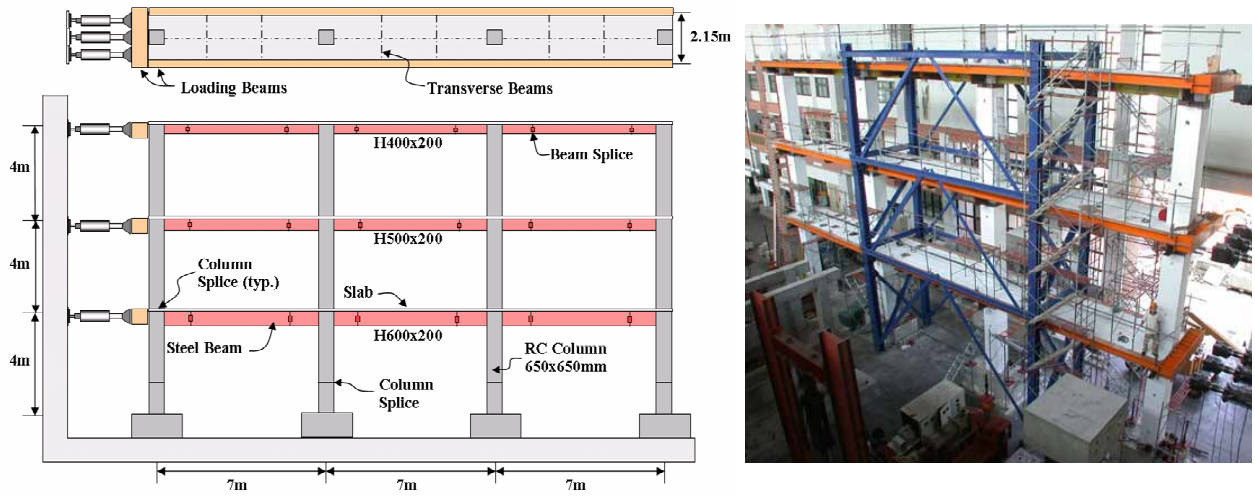

Figure 2 – Plan and elevation views and photo full-scale composite test frame

square meters per framing level).

The reinforced concrete columns of the frame are pre-cast with steel beam stubs and are field spliced using standard grouted sleeve couplers. As shown in Fig. 2, column splices at the base are located 1000mm above the footing and are flush with the slab above the first and second floors. Steel beams run continuous through the column and are spliced with bolted moment connections 1500 mm away from the column face. Bolted moment splices are designed per recommendations in FEMA 350 [19] to develop 1.2 times the expected moment strength at the column face. Further discussion of design considerations for the column and beam splices and their effect on behavior is discussed in the companion paper [3].

To capture the composite slab effect in the frame behavior, a 2150 mm wide composite floor slab is integrated with the main girder and the transverse beams on each level of the frame. The composite deck consists of 75 mm normal weight concrete slab over a 75 mm steel deck, with ribs running parallel to the frame. Three actuators, each with a capacity of 1000 kN and ±500 mm stroke, are installed at the each floor level. Loads are transmitted into the frame through stiff loading beams, which extend the entire length of the frame and are connected to the floor slab with horizontal shear studs and spiral reinforcement.

The frame was intentionally designed to the minimum limits of the building code provisions so as to represent the minimum expected performance and to interrogate system design parameters. As Taiwan's seismic design codes adopt similar requirements to those in the United States, the frame design is representative of building code standards in both countries.

Design Loading

The loading conditions for the design of the test frame are obtained from the International Building Code [2]. Typical office dead and live loads are assumed to be 4.4 and 2.4 kN/m^2 (92 and 50psf), respectively. The building is assumed to be located in a highly seismic area within either California or Taiwan, with seismic design forces based on mapped spectral accelerations of S_s = 1.5g and S_1 = 0.72g. The soil condition at the building site is assumed to be that of site class D (F_a = 1.0), and the building itself is assigned a Seismic Use Group I and a Seismic Design Category D. The building has a fundamental vibration period of 1.0 sec., as determined by the analytical model. This is in contrast to the value of 0.56 sec., which the IBC imposes as an upper bound for determining the design base shear. Using the code-specified period, the building lies in the constant acceleration portion of the design response spectrum. Based on the code spectrum, combined with other provisions (e.g., seismic response factor R = 8, provisions for accidental torsion, etc.), the frame has a design base shear coefficient of 0.13, which equates to a required base shear of 1160 kN.

Member Design

The steel beam designs are controlled by strength in negative bending, and therefore are sized based on their steel section properties. Shear studs are provided to develop the full composite beam strength in positive bending and to ensure adequate seismic force transfer between the slab and frame. The column design is governed by the strong-column weak-beam criterion (SCWB) of ACI 318 [10], which requires that the nominal column flexural strengths exceed 1.2 times the beam strengths framing into a joint. This applies at all floors except the top floor. The SCWB issue is critical to the frame design and is discussed in more detail in the companion paper [3]. Given the member sizes determined from the minimum strength and SCWB requirements, the drift criterion ($C_d \Delta_{el} = \Delta_{in} \leq 0.02$ (story height), with C_d = 5.5) was automatically satisfied and did not require any further resizing of the members. The member sizes and material strengths (including both minimum specified and measured strengths) are presented in Table 1.

Table 1 – Test frame member properties.

Floor	Steel Beams (d, b_f, t_w, t_f) $F_{y,nom}$ = 345 MPa ($F_{y,meas}$)	RC Columns	
		Section $f'_{c,meas}$=40 MPa ($f'_{c,meas}$)	Rein. Bars $F_{y,nom}$ = 415 MPa $F_{y,meas}$ = 527 MPa
1st	H600x200x11x17mm (426 MPa)	650x650mm (89 MPa)	Exterior 8-#11bars Interior 12-#11bars
2nd	H500x200x10x16mm (501 MPa)	650x650mm (68 MPa)	Exterior 4-#11bars Interior 12-#11bars
3rd	H396x199x7x11mm (419 MPa)	650x650mm (68 MPa)	Exterior 4-#11bars Int. Lower 12-#11bars Int. Upper 8#11bars

Beams are rolled shapes ranging in depths from 600 mm at the first floor to about 400 mm at the roof. Columns have reinforcing bar arrangements as shown in Fig. 1b, where the number of bars is adjusted to the minimum required based on strength requirements. As is apparent from Table 1, the measured material properties were found to be much higher than the nominal strengths used for design. This was particularly an issue in the second floor beams, where the material overstrength was in the range of 40%. This caused some concern since this had the potential to redistribute hinging from the beams into the columns, and possibly lead to a story mechanism. Its influence on the SCWB criterion is discussed in the companion paper [3]. The impact of this issue on the response of the frame is discussed in a later section.

Joint Design

As previously noted, the composite beam-column joints are designed following the ASCE Joint Recommendations [7] to develop M_p in the composite beams per the strong-joint weak-beam criterion in AISC Seismic Design Provisions [13]. The first and second floor joints utilize the standard joint details as shown in Fig. 1. Shown in Fig. 3 are diagrams of the idealized transfer mechanisms in the joint, which are mobilized by steel web stiffeners and band plates above and below the joint. Since space frames are common in Taiwan, it was decided to incorporate a transverse beam into the joints to simulate space frame conditions. This detail provides additional concrete confinement within the joint region and increases the strength and stiffness of the connection. The tie configuration for this joint was investigated during the subassembly stage of this testing program. The subassembly tests helped confirm we could avoid drilling holes within the beam webs and anchor the ties into the confined concrete between the two face bearing plates (see Fig. 1b).

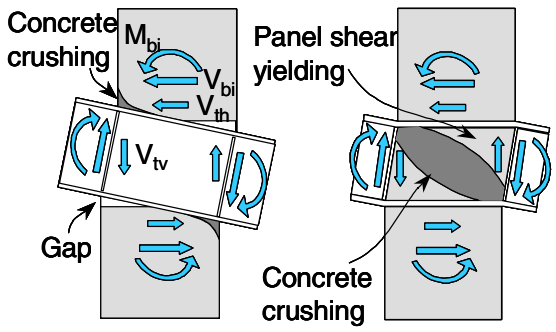

Fig. 3 Force transfer mechanisms in joint (after Kanno and Deierlein 2002)

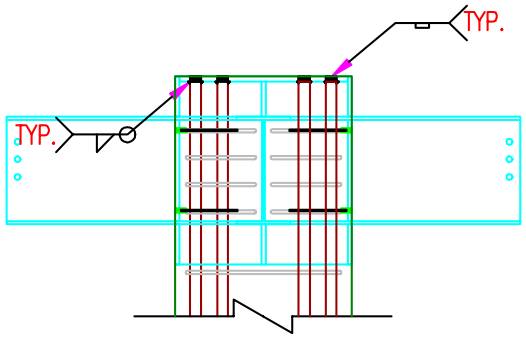

Fig. 4 Elevation of beam-column joint detail with steel cap plate at roof level

The top floor joints posed another complication, since the column does not extend above the joint and the standard force transfer mechanisms (Fig. 3) that for the basis of the ASCE Joint Recommendations [7] do not apply. Therefore, it was necessary to develop and evaluate a unique detail for this condition. Three alternative joint details were proposed and investigated through subassembly tests conducted in preparation for the full frame test. Based on this testing, we developed and used the cap plate detail shown in Fig. 4, which employs a steel plate on top of the column to provide anchorage for the longitudinal reinforcing bars and bearing force for the steel beam. As described later, like all the joints in the frame, this cap detail worked well and was able to develop beam hinging adjacent to the column with only minimal damage in the joint region.

Test Loading Protocol

Extensive nonlinear static and dynamic time-history analyses were performed using OpenSees [20] and PISA2D [21] prior to testing. These analyses were used to select suitable ground motions and investigate the most probable ultimate lateral strength and the inelastic demands imposed on the frame specimen under the simulated earthquake effects. The main focus of these studies was to predict the possible peak responses of the frame during the test while verifying that both the force and stroke limitations of the actuators were not exceeded. Ultimately, two earthquake records, TCU082-EW and LP89G04-NS, were

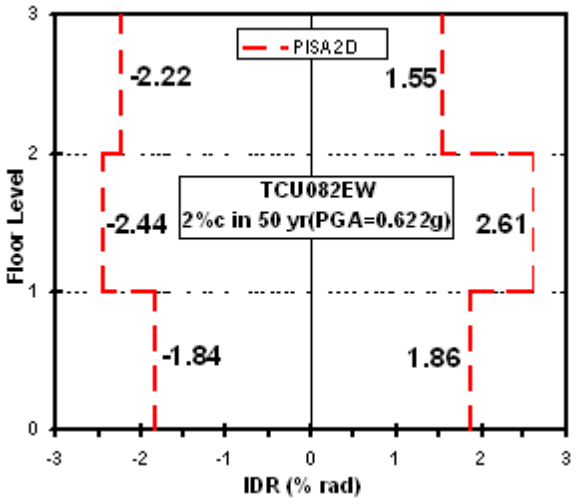

Figure 5 – The predicted peak interstory drift of test frame subjected to 2/50 TCU082.

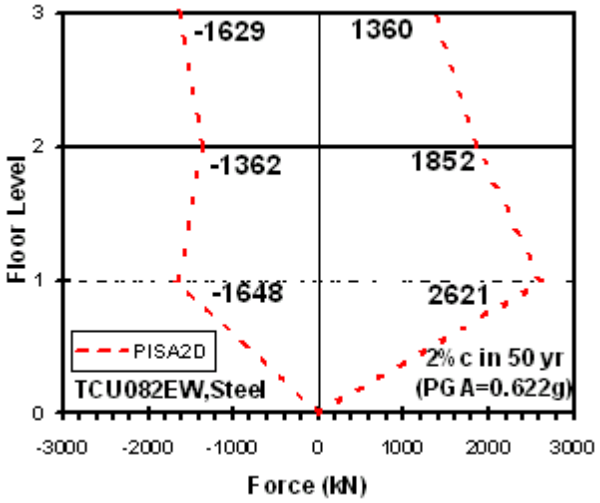

Figure 6 – The predicted peak story force required of actuators under the 2/50 TCU082.

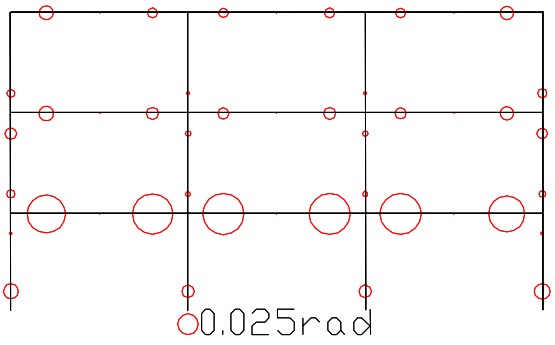

Figure 7 – Distribution of plastic hinges from 2/50 TCU082 as predicted by PISA2D

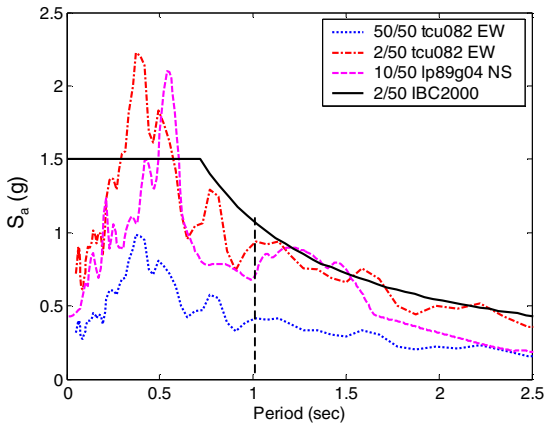

Figure 8 – Scaled response curves for earthquakes used in test simulation.

chosen from bins of the 1999 Chi-Chi and 1989 Loma Prieta earthquakes, respectively. Both OpenSees and PISA2D predicted that the peak responses from these events would be within the limitation of the actuators and suggested that the hinging was fairly well distributed in the frame. Figures 5 and 6 show the maximum interstory drifts and the peak story forces obtained from PISA2D for the TCU082 record scaled to a 2/50 hazard level. The estimated distribution and severity of plastic hinging are shown in Fig. 7.

Using the pseudo-dynamic loading methodology, these records are inputted as a series of four earthquake loading events, which are defined as follows: 50% chance of exceeding in 50 years (50/50) using a TCU082 record, then a 10/50 LP89G04 event, a 2/50 TCU082 event, and finally a 10/50 LP89G04 after shock. The scaled response spectrums for these events are shown in Fig. 8. After the four earthquakes, a final pushover using a triangular loading pattern was applied out to a roof drift ratio of 8%, with a corresponding maximum interstory drift of 10%.

For the pseudo-dynamic loadings, the records are scaled based on the spectral acceleration at the first mode period of the building to represent the range of different hazard levels. One important distinction to make here is that these hazard levels reflect a highly seismic Taiwanese site. The 10/50 event ($S_a(T_1)$=0.68g) matches that of the US site, but the 2/50 Taiwan event ($S_a(T_1)$=0.92g) is slightly less intense and corresponds to approximately a 4/50 hazard level for the US site. This is apparent from the differences between the 2/50 IBC2000 and 2/50 TCU082 response spectrum curve in Fig. 8 at a period of 1 second. The seismic mass used in the pseudo-dynamic algorithm is consistent with that used in the design, as is the gravity loads included into the geometric stiffness (P-Δ) effects.

Testing Techniques – ISEE

Internet-based Simulations for Earthquake Engineering (ISEE) has been developed by the researchers at NCREE as a prototype of Internet-based cooperative structural experimental environment [18]. During the full-scale RCS frame test, ISEE was activated to allow remote participants witness the real time video images of the specimen in the laboratory as well as the digital response data through the Internet. The schematic of the ISEE framework configured for this study is shown in Fig. 9. There are three major

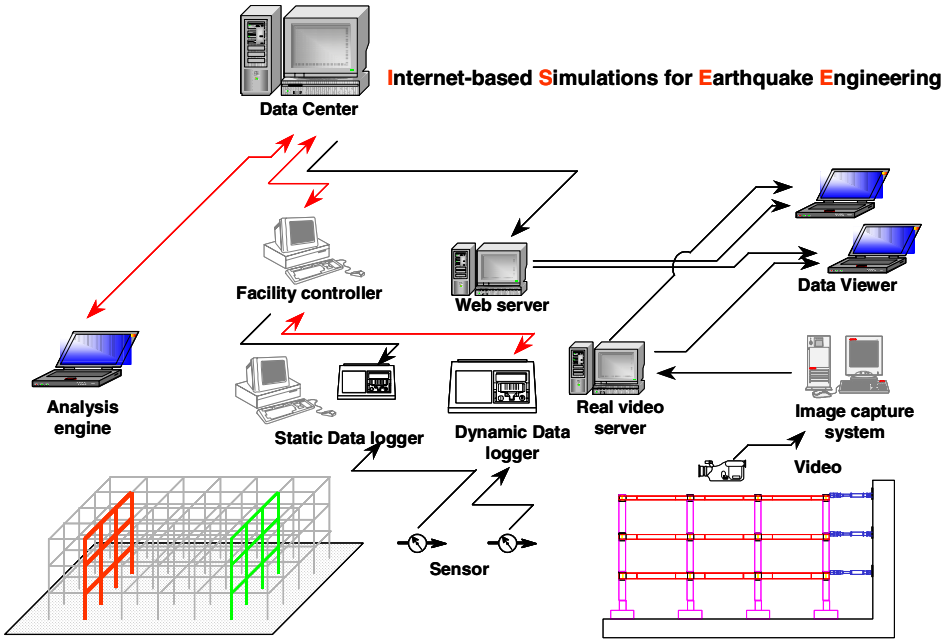

Figure 9 – ISEE framework employed in the pseudo-dynamic test

components in this framework: the Data Center, the Analysis Engine and the Facility Controller. The Data Center is a database server, which processes all the prescribed data sent from the Analysis Engine and the Facility Controller. The Analysis Engine handles the numerical integration of the dynamic responses of the entire system (analytical plus physical components) using Newmark explicit scheme with a time step size of 0.02 second. The Facility Controller is the software bridging the experimental facilities and the Data Center. When the target displacement is satisfactorily imposed, instruments record and send the data to the data logger while concurrently sending prescribed response data (floor displacements, story shears, etc.) back to the Data Center for real-time Internet distribution. The appropriate information is sent to the Analysis Engine to compute the target displacement for the next time step. An independent Real Video Server broadcasts the video images to allow data viewers witness the experimental responses in the laboratory.

CONSTRUCTION OF TEST SPECIMEN

The test frame was detailed and built in the precast method of construction in conformance with standard industry practice. This type of construction is commonplace in Taiwan and Japan, and therefore was method of choice for this test frame. This also provided the opportunity to test strength and toughness of the precast splice connections in the subassembly tests and the full-scale frame test, something which has not been widely investigated in RCS frames prior to this study.

Construction Process

At the precast fabrication plant, single story precast column assemblies were integrally cast with steel beam stubs to create a beam-column tree, as shown in Fig. 10a. The beam stubs are drilled and fabricated to accommodate the bolted splice connections to connect to the central beam spans. The lower region of the precast column is outfitted with standard mechanical couplers for the grouted splice connections. The upper region contains the embedded steel beam as well as the standard details shown in Figure 1. Longitudinal reinforcing bars protrude beyond the top of the column to allow for the grouted connection of the upper column. The foundation-column stub assemblies were prefabricated in the same manner.

The construction process began with the placement and anchorage of the foundation blocks, and followed by (1) installation of the beam-column trees, (2) erection and splicing of the steel beam spans, (3) erection and attachment of the loading beams and the transverse beams, (4) plumbing of the story followed by tightening of the steel bolts and grouting of the column splices, and (5) the layout and attachment of the steel deck. This process was repeated until all three floors were completed, with each floor requiring about two days work. Figure 10b is a photo of the unfinished frame as workers begin construction on the second floor. Once the full frame was constructed, workers attached shear studs to the floor beams, laid out the wire mesh reinforcement, and poured the slab. The finished slab marked the completion of the frame construction. The entire specimen was constructed in the NCREE lab within two weeks from the positioning of the pre-cast footings to pouring of concrete slabs.

(a) (b)

Figure 10 – Construction photos of (a) a typical pre-cast beam-column module and (b) construction of the 2nd floor.

TEST FRAME RESULTS

The frame test was conducted in October of 2002 and was witnessed by about thirty researchers from the US, Taiwan, and Japan. Testing was broadcasted live via the Internet (http://rcs.ncree.gov.tw), including real-time data plots and live video. The response of the frame was monitored and documented with over 300 data channels, visual inspections, and photographic images.

Description of General Response and Damage

Examples of the recorded test results during the earthquake portion of the loading history are shown in Figure 11, which includes plots of the roof displacement history throughout all events (Fig. 11a), the maximum and minimum interstory drift ratios (Fig. 11b), and the maximum and minimum story shears (Fig. 11c). The following discussion is a brief overview of the general response of the frame and a description of the damage patterns after each of the loading events.

EQ#1 – 50% in 50 year: During this event the roof experienced a maximum displacement of about 200mm, with fairly uniform interstory drift values that ranged from 1.5 to 2.0%. A maximum base shear of about 3000kN was reached during this event, which is about 2.6 times that of the design value (1160kN). The residual drifts after the event were negligible. There were very minor cracks observed

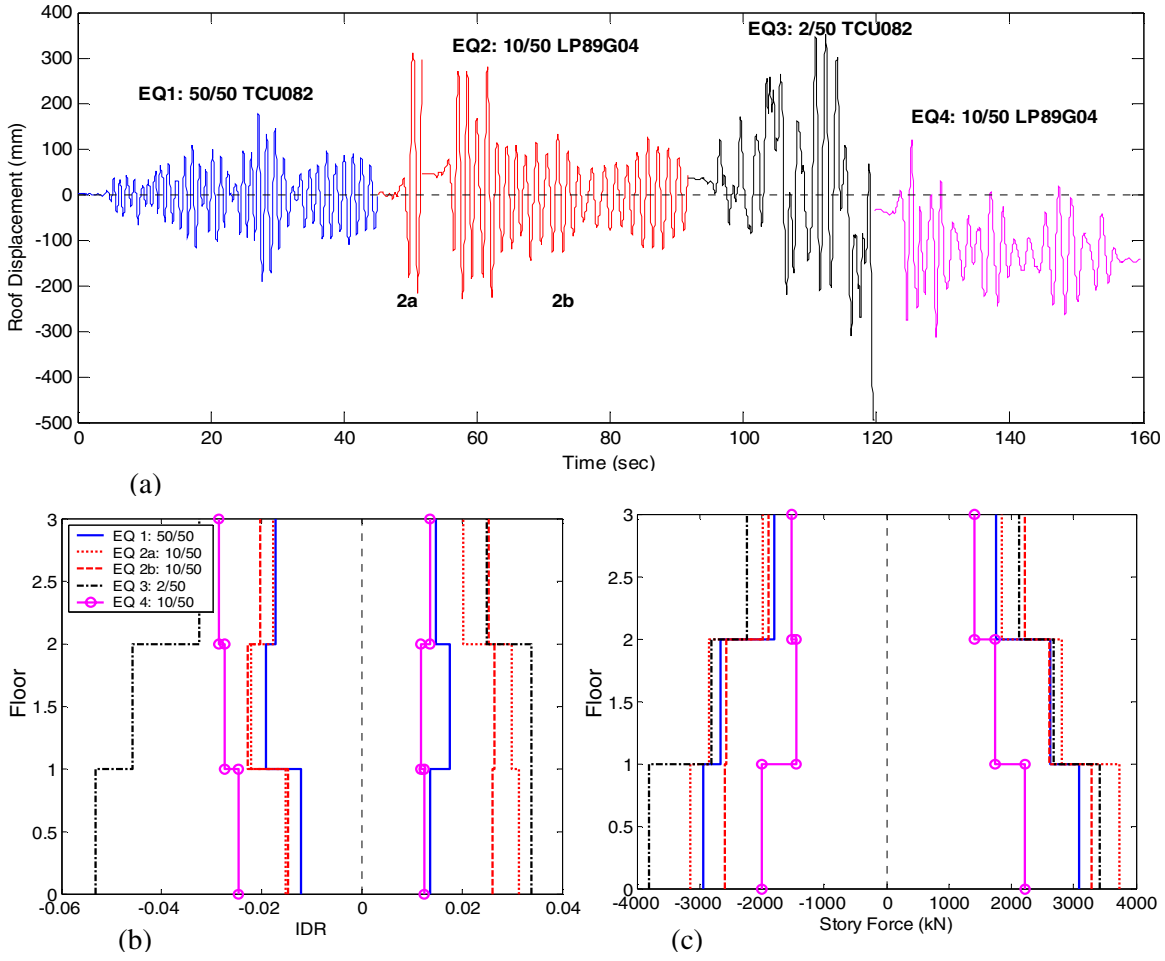

Figure 11 – Global response of frame to earthquake excitations. (a) Roof displacement, (b) Max/min IDR, and (c) Story force.

within the first floor reinforced concrete columns at the base, some minor yielding of the steel beams, and virtually no damage to the concrete slab or composite joints. During this test, and throughout all subsequent tests, there was loud bolt-banging, associated with slippage of bolts in the beam splices. Aside from the loud sound, the bolt slippage and banging did not detrimentally affect the frame. Upon thorough inspection following the loading, researchers and engineers witnessing the test agreed that the frame met performance target for "immediate occupancy", where the structural stability was not compromised and the frame required little if any repair.

EQ#2 – 10% in 50 year: Due to a problem with the out-of-plane bracing, the first design level event (10/50 LP89G04) had to be stopped at about 7 seconds into the record and then restarted from the beginning. This first segment of this event (see 2a in Fig. 11a) pushed the frame out to 3% interstory drift and began to cause some visible hinging at the column bases. The resulting loss of stiffness at the base columns triggered an unexpected failure in the lateral bracing frame, which permitted the RCS frame to rock out-of-plane to a roof drift of about 1.5%. Thus, in addition to base hinging associated with the in-plane drift of about 3%, the column bases experienced some additional out-of-plane hinging associated with the 1.5% out-of-plane drift. After surveying the damage, the out-of-plane bracing was repaired to permit restarting the 10/50 earthquake event. However, being as the frame had already experienced the major excursions of the first 10/50 event (segment 2a), it was decided to rerun the 10/50 event scaled down to 80% of its original intensity. This was done with the assumption that the two events (segments 2a and 2b) would represent the intensity and damage equivalent to that which would be imposed by the full 10/50 design level event. Ultimately, the maximum roof displacement that occurred during this design level event was about 300mm, with maximum interstory drifts ranging from 1.5% to 3.0%. The base shear was approximately 3800kN, which is about 3.3 times larger than the design base shear; and the residual roof drift was approximately 0.3%.

After the completion of this event, crack widths near the base of the 1st floor columns opened to about 2 mm and were accompanied by some minor spalling of the cover concrete (see Fig. 12a). Minor hairline cracks also appeared in the upper portion of the second floor columns, with some minor spalling beneath the joint's steel band plate (Fig. 12b). The steel beams in all floors yielded (see Fig. 13a, 13b), although the second floor beams experienced much less yielding than the other stories (Fig 12b). Local buckles appeared in the first and third story beams in the lower flanges and slightly into the web (Fig. 13a). The largest buckling distortions at the flange tips measured up to 15 to 25 mm, which occurred at the first and thrid floor beams framing into the exterior joints. There was some minor yielding in the lower flange beam splice plates in the central bay of the first floor beams. The composite joints experienced very minor cracking (Fig 12b, 13b). The first and second floor slabs experienced some minor cracking along the length of the frame, but in general the slab was still very much intact. At this stage, the building was considered to meet the "life safety" performance target, where the level of damage required repairs but had not significantly affected the safety of the structure. Repairs to the structure would likely involve epoxy injection of cracks, patching of spalled concrete, heat straightening of local flange buckles, and plumbing to reduce residual interstory drift.

EQ#3 – 2% in 50 year: Under the 2% in 50 year event, assumed to represent the so-called maximum considered earthquake, the frame experienced a maximum roof displacement of 500 mm at about 28 seconds into the record. This displacement corresponds to the maximum stroke allowed by the actuators, which prevented the pseudo-dynamic loading to continue beyond this point. Examination of the pseudo-velocities and accelerations at this point suggested that the frame had reached its maximum drift and was beginning to return back. Analytical simulations (presented in the companion paper) further confirmed that this was the maximum excursion of the event and that subsequent cycles were smaller. Given this information, it was decided that the loading up to this point represented the main features of the maximum considered event (2/50) even though it was subjected to only 28 of the full 45 seconds. During this event, deformations began to concentrate in the first two stories, with a maximum IDR of 5.5% occurring in the

(a) (b) (c) (d)

Figure 12 – Typical conditions of the base columns and the 2nd floor beam-column joint following (a, b) the design level and (c, d) the maximum considered earthquakes.

(a) (b) (c) (d)

Figure 13 – Typical conditions of exterior beam (1B1S) and interior beam/composite joint (1J3) following (a, b) the design level and (c, d) the maximum considered earthquakes.

first floor. The maximum base shear remained about 3800kN. The residual roof drift after this event was about 2.7%, with the largest contribution from the first floor (3.4%).

This record caused significant hinging within the base of the first floor columns, which resulted in distributed cracks up to 5 mm in width and significant spalling of the cover concrete (Fig. 12c). In addition, large cracks measuring about 10 mm opened up between the bottom of the column and the footing - presumably due to yield penetration of the longitudinal bars in the column footing. The flexural cracks within the upper region of the second floor columns grew to widths of 4 mm and were accompanied by minor spalling just below the beam-column joint (Fig. 12d). The second floor beams exhibited only slight yielding beyond that observed under EQ#2 as the inelastic deformations began to concentrate in the columns directly beneath the beams (Fig. 12d). The first and third floor beams experienced extensive yielding, with flange yield penetrations reaching as far as 1.25 times the depth of the beam (Fig. 13d). The local buckles also became more severe within these beams, concentrating in the bottom flanges and the lower half of the web, with flange tip distortions up to 70 mm (Fig. 13c). The first and second floor slabs experienced some local crushing on the interface of the slab and the column, as well as cracking, which occurred on all three floors. The composite joint regions remained relatively undamaged, experiencing only minor cracking (Fig. 12d, 13d). With significant local damage and a residual interstory drift of 3.4% (140 mm) in the first story, the consensus of participants at the test was that the frame had reached its “collapse prevention” performance level, implying that the structure would need significant repairs to restore its strength and stiffness.

EQ#4 – 10% in 50 year: Given the large amount of residual drift after the 2/50 event, there was concern that the frame would again hit the maximum actuator stroke the final 10/50 event. Therefore the decision was made to straighten the building as much as possible before continuing. This realignment was done using the actuators and reduced the residual roof drift to approximately 0.3%. The final pseudo-dynamic event was then run, which involved re-running the 10/50 design level event. Here the decision was made to repeat the scaled (80%) version of the 10/50 event, so as to repeat the record used for loading segment 2b (see Fig. 11a). Thus, this event had two purposes. One was to help gage the amount of damage caused by the 2/50 (maximum considered) earthquake. The second was to simulate the effects of an aftershock to the 2/50 event. The maximum roof drift during this record was about 300mm, with interstory drifts remaining within 3%. The base shear was considerably lower in this event than in the previous three, with values peaking at approximately 2200kN, presumably due to the softening under the multiple earthquakes. The residual roof drift was about 1.1%. The post event inspection revealed little additional damage beyond that observed after the maximum considered (2/50) event.

Final Static Pushover: The final pushover of the frame resulted in a maximum base shear of 3200kN (Figure 14), which is about 2.8 times that of the design base shear. This reveals that even after sustaining significant damage through four major earthquakes, the frame still maintained a very large overstrength. It was necessary to complete the pushover in two stages so that the actuators could be readjusted to accommodate the large drifts. This is apparent in the unloading-reloading sequence that occurs at about 5% drift in Fig. 14. During this test, deformations continued to concentrate in the first and second floors, creating a fairly pronounced two-story mechanism, characterized by column hinging at the base and beneath the second floor beams and flexural yielding of the first floor beams. The second floor beams were found to have measured yield strengths 40% larger than the specified minimum strength (484 MPa versus the minimum specified yield strength of 345 MPa), which led to limited yielding in the second floor beams and hinging in the columns.

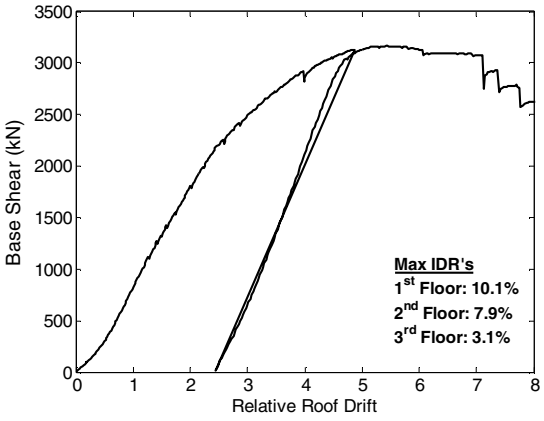

Figure 14 – Final pushover

Concentration of deformations in the lower two stories of the frame resulted in a peak interstory drift ratio of 10% in the first story. As shown by the middle photo in Fig. 15, by the conclusion of the test, there was severe hinging at the column bases, with extensive cracking, spalling, and crushing of the concrete. The concrete was fully deteriorated in this region and the rebars were primarily acting in dowel action to carry the large amount of shear transmitted through these columns. There was significant yielding and local buckling in the first floor beams (see the left photo in Fig. 15) with beam flange distortions in the exterior joint reaching approximately 90 mm. The upper hinges at the second floor columns experienced flexural cracks up to 8 mm wide and developed a 10mm gap below the joint's steel band plate. The sudden strength drop apparent in Fig. 14 at a roof drift ratio of 7% (corresponding to about 9% interstory drift in the first story) was caused by a net section rupture in one of the lower beam flange splice plates for one of the first floor beam splices. This is shown in the right photo of Fig. 15. This first rupture precipitated subsequent ruptures in neighboring splices, which are evident in the strength drops under continued loading (see Fig. 14). Note that the beam splices were designed to develop the shear and moment associated with the expected strength of the beams at the column face, which turned out to be just about equal the actual plastic beam moment based on the measured steel yield strength. The splice fracture is not considered a serious concern, given that it only occurred after 10% story drift with significant distortions in the first-floor framing.

Figure 15 Condition of beam-column joint, RC column base, and bolted beam splice at end of static pushover to 10% interstory drift

General Observations

The concrete slab performed surprisingly well throughout the entire loading protocol. It was expected that there would be much more concrete crushing and more severe cracking that would compromise the integrity of the slab. Instrumentation confirmed that the slab did not slip or pull off of the beam, and subsequent dismantling of the slab showed no evidence of shear stud fracture. This is in stark contrast to the subassembly tests that were performed earlier in this program, which demonstrated quick deterioration of the slab and the shear studs.

Throughout the test, local buckling of the steel beam was concentrated in the lower beam flange and the lower portion of the web. It was evident that the slab provided adequate restraint to prevent distortions from developing in the upper flanges. It was also apparent that the most severe buckling took place at the beam hinges framing into the exterior joints. It seems that the continuity of the beam and the slab in the interior joints provided additional restraint which did not allow the level of buckling that was occurring at the exterior joints. In addition to this, it was common to see large buckles form in the beam hinging zones during one loading excursion, only to be straightened out later when the earthquake produced an excursion in the opposite direction. These are particularly interesting issues because they do not arise within most subassembly tests, which points to the difficulty and unresolved error in modeling the boundary conditions in typical beam-column tests.

The composite joints behaved very well throughout all phases of the loading protocol. Even through the final pushover, the composite joints, with typical standard details, experienced only minor to moderate cracking and forced hinging to occur in the steel beams.

The RC column base hinges were subjected to significant plastic rotations throughout the loading history of the test frame. As a result, the concrete within these hinges was significantly deteriorated to the point that during the final pushover test the rebars were carrying nearly all the moment and shear. This type of behavior seemed to be a result of a combination of extensive plastic hinging and progressive shear failure. If the beam splices had not failed, it is reasonable to state that the test would have been stopped shortly thereafter due to the severity of damage within these columns.

CONCLUSIONS

Past studies have demonstrated that when RCS composite moment frames are designed to current standards, they have the strength, stiffness, and ductility required to safely resist large earthquakes and are comparable to the performance of steel or reinforced concrete frames. Prior research has shown that the

beam-column connections can be detailed in a very simple and practical manner to provide sufficient strength and reliable seismic behavior. The full-scale RCS frame tested at the NCREE laboratory further validates the reliability of this innovative system. Designed to just meet the minimum requirements of current building code standards, the full-scale frame performed very well under four earthquake loading scenarios and a final pushover test out to an interstory drift ratio of 10%. Composite beam-column joints designed with standard details exhibited excellent behavior, as did the precast column splices. Overall, the test frame clearly demonstrates the capabilities of composite moment frames to meet and exceed the seismic performance expectations implied by modern building codes. In a companion paper [3] the design implications of this test as well as validation of the nonlinear simulation models are further explored.

ACKNOWLEDGEMENTS

The authors gratefully acknowledge support to plan and conduct the full-scale composite frame test from the National Science Council (NSC91-2711-3-319-200-14) and the National Center for Research in Earthquake Engineering (NCREE) of Taiwan. In particular, Mr. Kung-Juin Wang successfully implemented and executed the pseudo dynamic test software. Mr. Wei-Chung Cheng constructed the web servers for on-line data and video display. Additional support for planning and analyzing the test was provided by the National Science Foundation (Award Number CMS – 9975501) and the Pacific Earthquake Engineering Research Center (Award Number EEC-9701568). Also acknowledged are the management, research and technical staff at NCREE and the Ruentex Construction and Development Company. Any opinions, findings, or other conclusion or recommendations expressed in this material are those of the authors and do not necessarily reflect those of the sponsors and contributors.

REFERENCES

1. Deierlein, G.G., Noguchi, H. (2004), “Overview of US-Japan Research on the Seismic Design of Composite Reinforced Concrete and Steel Moment Frame Structures,” *JSE*, ASCE, 130(2), pp. 361-367.
2. ICC (2000), “International Building Code,” *Inter. Code Council*, Falls Church, VA, April 2000.
3. Cordova, P., Chen, C.H., Lai, W.C., Deierlein, G.G. and Tsai, K.C., “Pseudo-Dynamic Test of Full-Scale RCS Frame: Part 2 – Analyses and Design Implications,” *Proceedings of 13th World Conference on Earthquake Engineering*, Paper #674, Vancouver, Aug. 2004.
4. Griffis, L.G. (1992), "Composite Frame Construction," *Constructional Steel Design - An Int. Guide*, Ed. Dowling, Harding, Bjorhovde, Elsevier Applied Science, NY, pp. 523-554.
5. Sheikh, T.M., Deierlein, G.G., Yura, J.A., Jirsa, J.O., (1989), “Beam-column moment connections for composite frames: Part 1,” *JSE*, ASCE, 115(11), 2858-2876.
6. Deierlein, G.G., Sheikh, T.M., Yura, J.A., and Jirsa, J.O. (1989), “Beam-column moment connections for composite frames: Part 2,” *JSE*, ASCE, 115(11), pp. 2877-2896.
7. ASCE (1994), “Guidelines for design of joints between steel beams and reinforced concrete columns,” *JSE*, ASCE, 120(8), 2330-2357.
8. Kanno, R. and Deierlein, G.G. (2002), “Design Model of Joints for RCS Frames,” *Composite Const. in Steel and Concrete IV*, ASCE, pp. 947-958.
9. Parra-Montesinos, G., Wight, J.K. (2001), “Modeling Shear Behavior of Hybrid RCS Beam-Column Connections,” *JSE*, ASCE, 127(1), pp. 3-11.
10. ACI (2002), *Building Code Requirements for Structural Concrete*, ACI-318-02, American Concrete Institute, Farmington Hills, MI.
11. AISC (1999), *Load and Resistance Design Specification for Structural Steel Buildings*, 2nd Ed., American Institute of Steel Construction, Chicago, IL.
12. ASCE (2002), “Minimum Design Loads for Buildings and Other Structures,” *SEI/ASCE 7-02*, ASCE, Reston, VA.

13. AISC (2002), *Seismic Provisions for Structural Steel Buildings*, American Inst. of Steel Construction, Chicago, IL
14. Deierlein, G.G. (2000), "New Provisions for the Seismic Design of Composite and Hybrid Structures" *Earthquake Spectra*, EERI, 16(1), pp. 163-178.
15. Kanno, R. (1993), "Strength, Deformation, and Seismic Resistance of Joints between Steel Beams and Reinforced Concrete Columns," *Ph.D. Thesis*, Cornell University, Ithaca, NY.
16. Mehanny, S.S.F., Deierlein, G.G. (2001), "Seismic Damage Analysis – Assessing Collapse Prevention for Composite Moment Frames," *JSE*, ASCE 127 (9) pg. 1045-1053.
17. Hsieh, S.H., Tsai, K.C., Yang, Y.S., Wang, K.J., Hsu, J.W., Wang, S.J., Loh, C.H. (2002), "An Internet-based Environment for Collaborative Networked Pseudo Dynamic Tests," *Proceedings*, *the 4th Seminar on Earthquake Engineering for Building Structures*, Seoul, Oct.
18. Yang, Y. S., Hsieh, S. H., Wang, K. J., Wang, S. J., Hsu, C. W., and Tsai, K. C. (2002), "Numerical Analysis Framework for Distributed Pseudo-Dynamic Tests," *Proceedings of the 2nd International Conference on Structural Stability and Dynamics,* Singapore.
19. FEMA-350 (2000), "Recommended Seismic Design Criteria for New Steel Moment-Frame Buildings," SAC Joint Venture (funded by Federal Emergency Management Agency), June 2000
20. McKenna, F., and G. L. Fenves (1999), "G3 Class Interface Specification Version 0.1 – Preliminary Draft," Pacific Earthquake Engineering Research Center, University of California at Berkeley, USA
21. Tsai, K.C., Chang, L.C., "The Platform and Visualization of Inelastic Structural Analysis of 2D Systems PISA2D and VISA2D," Report No. CEER/R90-08, Center for Earthquake Engineering Research, National Taiwan University. (in Chinese), 2001.